In Situ Polymerization of Aniline Sulfonic Acid Derivatives into LDH Interlamellar Space Probed by ESR and Electrochemical Studies

El Mostafa Moujahid, Marc Dubois,* Jean-Pierre Besse, and Fabrice Leroux*

Laboratoire des Matériaux Inorganiques, CNRS-UMR no. 6002, Université Blaise Pascal, 63177 Aubière cédex, France

Received May 13, 2004. Revised Manuscript Received October 18, 2004

Aniline sulfonic acid derivatives, *o*- and *m*-aminobenzenesulfonic, 3-amino-4-methoxybenzenesulfonic, 3-aniline-1-propane sulfonic acid, and 4-aniline-1-butane sulfonic acids, are incorporated via direct coprecipitation between the sheets of a layered double hydroxide (LDH) of intralamellar composition $Cu_2Cr(OH)_6$. After a subsequent thermal treatment at 200 °C applied under air to the hybrid materials, the degree of connectivity between guest monomers, i.e. dimerization and/or polymerization, is evaluated by ESR spectroscopy. Additionally, the hybrid phases were electrochemically cycled in a nonaqueous protophobic electrolyte. The redox potentials are discussed as a function of the position of $-NH_2$ amino group and of $-OCH_3$ electron donating group located in the benzene ring and of the presence of the pendent alkyl chain attached to the nitrogen atom.

1. Introduction

A lot of attention is devoted to the preparation of multifunctional materials. For two decades, 2D-hybrid materials composed of a polymer and an inorganic host structure have been extensively studied.[1] Indeed these materials may provide mixed properties arising from the two parts, the lamellar host structure supplies a constrained environment in which the polymer is forced to locate and both parts may also act synergistically.

In different fields of application, enhancement of the electronic conductivity has been a leitmotiv for these alternated lamellar systems. Polyaniline (PANI) which exhibits a good electronic conductivity, but associated to a rather poor processability, has been and is still extensively studied as an organic component for 2D-nanocomposites. It was exemplified with several 2D host materials such as V_2O_5 xerogel,[2] Na_xMoO_3 bronze,[3] α-$RuCl_3$,[4] $VOPO_4 \cdot H_2O$,[5] layered perovskites $HCa_2Nb_3O_{10}$ and $HCa_2Nb_2MO_9$ (M = Al, Fe),[6] or Brönsted acids $HMMoO_6 \cdot H_2O$ (M = Nb, Ta),[7] etc. One has to note the incorporation of (PANI) into 3D host framework such as MCM41[8] and zeolite[9] or its encapsulation of 0D systems such as of nanometer-size particles of TiO_2 for application in photoconduction.[10] Other approaches were used for the preparation of PANI such as emulsion methods or mixtures with aniline derivatives in order to increase the processability and the pH domain in which the polymer is conductive as well.[11] PANI was also associated with clay minerals; the assembly is then called a polymer clay nanocomposite (PCN).[12] The electropolymerization of aniline has been attempted into montmorillonite;[12(a)] it was also found that PCN materials offer good corrosion protection better than conventional PANI coating and present a drastic decrease as O_2 gas barrier.[12(b)] Concerning anionic clays, few recent works report the in situ polymerization of aniline-related monomer in the interlayer gap.[13] The so-called layered double hydroxide (LDH) materials are known to provide some potential applications as clay-modified electrodes after the encapsulation of electroactive molecules.[14] Hydrotalcite-like LDH materials are described according to the ideal formula, $[M^{II}_{1-x}M_x^{III}(OH)_2]^{x+}_{intra}[A^{m-}_{x/m} \cdot nH_2O]_{inter}$, where M^{II} and M^{III} are metallic cations, A is the anions, and intra and inter denote the intralayer and interlayer domain, respectively. The structure consists of brucite-like layers constituted of edge-sharing octahedra. The presence of trivalent cations

* Authors to whom correspondence should be addressed. E-mail: mdubois@chimtp.univ-bpclermont.fr; fleroux@chimtp-univ.bpclermont.fr.

(1) (a) Komarni, S. *J. Mater. Chem.* **1992**, *2*, 1219. Ruiz-Hittzky, E. *Adv. Mater.* **1993**, *5*, 334. (b) Giannelis, E. *Adv. Mater.* **1996**, *8*, 29. Novak, B. M. *Adv. Mater.* **1993**, *5*, 422. (c) Ishida, H.; Campbell, S.; Blackwell, J. *Chem. Mater.* **2000**, *12*, 1260. (d) Leroux, F.; Besse, J.-P. *Chem. Mater.* **2001**, *13*, 3507.
(2) Kanatzidis, M. G.; Wu, C.-G.; Marcy, H. O.; Kannewurf, C. R. *J. Am. Chem. Soc.* **1989**, *111*, 4139.
(3) Kerr, T. A.; Wu, H.; Nazar, L. F. *Chem. Mater.* **1996**, *8*, 2005.
(4) Wang, L.; Brazis, P.; Rocci, M.; Kannewurf, C. R.; Kanatzidis, M. G. *Chem. Mater.* **1998**, *10*, 3298.
(5) Kinomura, N.; Toyama, T.; Kumada, N. *Solid State Ionics* **1995**, *78*, 281.
(6) Gopalakrishnan, J. *Mater. Sci. Eng. B* **1995**, *34*, 175.
(7) Bhuvanesh, N. S. P.; Gopalakrishnan, J. *Mater. Sci. Eng. B* **1998**, *53*, 267.
(8) Enzel, P.; Bein, T. J. *J. Phys. Chem.* **1989**, *93*, 6270.
(9) Frisch, H. L.; Song, H.; Ma, J.; Rafailovich, M.; Zhu, S.; Yang, N.-L.; Yan, X. *J. Phys. Chem. B* **2001**, *105*, 11901.
(10) Feng, W.; Sun, E.; Fujii, A.; Wu, H.; Niihar, K.; Yoshino, K. *Bull. Chem. Soc. Jpn.* **2000**, *732*, 627.
(11) Kuramoto, N.; Geniès, E. M. *Synth. Met.* **1995**, *68*, 191.
(12) Inoue, H.; Yoneyama, H. *J. Electroanal. Chem.* **1987**, *233*, 291. Yeh, J.-M.; Liou, S.-J.; Lai, C.-Y.; Wu, P. C.; Tsai, T.-Y. *Chem. Mater.* **2001**, *13*, 1131.
(13) (a) Challier, T.; Slade, R. C. T. *J. Mater. Chem.* **1994**, *4*, 367. (b) Isupov, V. P.; Chupakhina, L. E.; Ozerova, M. A.; Kostrovsky, V. G.; Poluboyarov, V. A. *Solid State Ionics* **2001**, *141−142*, 231. (c) Moujahid, El M.; Dubois, M.; Besse, J.-P.; Leroux, F. *Chem. Mater.* **2002**, *14*, 3799.
(14) Chibwe, M.; Pinnavaia, T. J. *J. Chem. Soc., Chem. Commun.* **1993**, 278.

10.1021/cm0401701 CCC: $30.25
Published on Web 12/21/2004

induces a positive charge in the layers, which is counterbalanced by interlamellar anions. Large anions such as polyoxometalate,[15] DNA molecule,[16] and biopolymer[17] have been intercalated between the LDH sheets.

To incorporate functionalized aniline-based polymer, sulfonate-derived aniline was preferred rather than the sulfonation on the formed polymer because the latter method gives rise generally to nonfully sulfonated polymer,[18] and the incorporation of preformed polymer may be hampered by diffusion.

We have shown recently that the polymerization reaction may occur in the gallery of hydrotalcite-type compound $Cu_2Cr(OH)_6Cl{\cdot}H_2O$ for the monomer derivative 3-aminobenzene sulfonate, under mild conditions,[13c] although the oxidative polymerization of bulk aniline sulfonate requires high pressure (19 kbar) and the presence of external oxidative agent.[19] This underlined the importance of the confinement provided by LDH structure.

Taking treatment conditions similar to those reported in our previous paper, and with the idea that the degree of polymerization between monomers may be partially governed by spatial occupancy, we studied the effect of the sulfonate group position attached to aniline and the presence of an additional electron withdrawing group, $-OCH_3$, on the benzene ring. In the same idea, two additional molecules fonctionalized by sulfonate end group and having an alkyl chain spacer were employed to potentially improve the connectivity by slight twist motion. It is known that alkane sulfonic substitute will induce additional deformation along the polymer, moreover its electron donating effect should stabilize radical cations.[20] Such self-doped polyaniline derivatives were found to form liquid crystalline solution.[21] Poly(aniline-*N*-butylsulfonate) was studied for its electrochromic properties,[22] and poly(aniline-*N*-propane sulfonic acid) was incorporated between xerogel V_2O_5 sheets.[23] The hybrid phase is found to be more electronic conducting than the pristine inorganic framework and to present shorter ionic diffusion pathways, as previously underlined on other relative systems (PANI)/V_2O_5.[24]

The inorganic−organic assemblies were characterized by means of X-ray diffraction and electron spin resonance (ESR) spectroscopy (both techniques were performed in in situ conditions as a function of the temperature) and the electrochemical behavior of the nanocomposites was tested in nonaqueous electrolyte. The comparison between as-obtained and thermally treated samples allows us to conclude on the redox activity arising from the polymer chains or dimers formed during the thermal treatment or produced upon electrochemical cycling.

Finally, based on structural considerations and the results gathered experimentally, some models are proposed to explain the degree of connectivity of the constrained molecules.

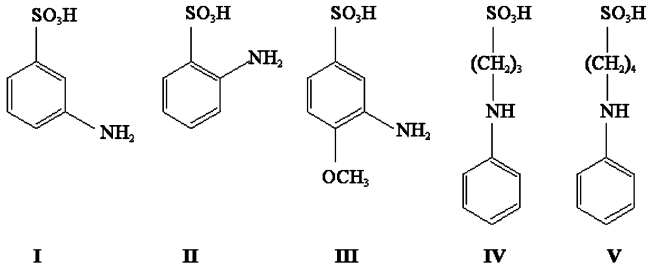

Figure 1. Representation of the monomers.

2. Experimental Section

Chemicals. Metanilic acid (*m*-aminobenzenesulfonic acid, 97%, Aldrich), aniline-2-sulfonic acid (Aldrich, 95%), 3-amino-4-methoxybenzenesulfonic acid (Acros, 98%), acetonitrile (Aldrich, $d = 0.786$), $CuCl_2{\cdot}2H_2O$ (Prolabo, >99%), $CrCl_3{\cdot}6H_2O$ (Fluka, >98%), and NaOH (Acros, >97%) were used as received.

Preparation of the Alkane Sultone Aniline Molecules. The reaction of alkane sultone aniline is based on a nucleophile attack of the nitrogen on the bonding C−O of the sultone, the sulfonic acid group is introduced together with the alkyl chain. The preparation is described in the literature.[25]

To prepare 3-aniline-1-propane sulfonic acid, 3.9 g of 1,3-propanesultone ($C_3H_6O_3S$, Fluka, ≥98%) was added to 4.46 g of aniline (Acros, 99.8%) into a benzene solution (Acros, $d = 0.879$) of 150 mL. The solution was then refluxed at 86 °C for 6 h. A white precipitate was formed which was recrystallized in ethanol solution.

To prepare 4-aniline-1-butane sulfonic acid, 2.723 g of 1,4-butane sultone ($C_4H_8O_3S$, Acros, ≥99%) was added to 4.655 g of aniline in a solution of 30 mL of acetonitrile. The solution was refluxed at 100 °C for 12 h.

Elemental analyses (C, S, N, and H) performed at the Vernaison Analysis Center of CNRS were in agreement with chemical formulas of the two organic molecules.

Hybrid Materials. The incorporation of organic molecules was performed using the "organized assembly" method. The amount of organic dispersed in aqueous solution corresponds to twice the LDH exchange capacity surmising the complete reaction of the metal chloride salts. Experimentally, a solution with 0.170 g of $CuCl_2$ (10^{-2} M) and 0.133 g of $CrCl_3$ ($5{\cdot}10^{-3}$ M) was added to an aqueous solution containing 10^{-2} M of dissolved organic molecules, 1.73 g for *m*- and *o*-aminobenzenesulfonate (**I** and **II**, respectively), 2.03 g for 3-amino-4-methoxybenzenesulfonic (**III**), 2.14 g for 3-aniline-1-propane sulfonic acid (**IV**), and 2.28 g for 4-aniline-1-butane sulfonic (**V**). The organic molecules are displayed in Figure 1.

The addition performed under nitrogen atmosphere and at constant pH of 5.5 using NaOH was complete after 24 h. The slurry

(15) Narita, E.; Kaviratna, P.; Pinnavaia, T. J. *Chem. Lett.* **1991**, 805.
(16) Choy, J.-H.; Kwak, S.-Y.; Park, J.-S.; Jeong, Y.-J.; Portier, J. *J. Am. Chem. Soc*. **1999**, *121*, 1399.
(17) (a) Whilton, N. T.; Vickers, P. J.; Mann, S. *J. Mater. Chem*. **1997**, *7*, 1623, (b) Leroux, F.; Gachon, J.; Besse, J.-P. *J. Solid State Chem*. **2004**, *177*, 245.
(18) Chen, S. A.; Hwang, G. W. *Macromolecules* **1996**, *29*, 3950. Wei, X.; Epstein, A. J. *Synth. Met.* **1995**, *74*, 123. Yue, J.; Wang, Z. H.; Cromack, K. R.; Epstein, A. J.; MacDiarmid, A. G. *J. Am. Chem. Soc.* **1991**, *113*, 2665.
(19) Chan, H. S. O.; Neuendorf, A. J.; Ng, S. C.; Wong, P. M. L.; Young, D. J. *J. Chem. Soc., Chem. Commun.* **1998**, 1327.
(20) Chen, S. A.; Hwang, G. W. *J. Am. Chem. Soc.* **1995**, *117*, 10055.
(21) Kim, E.; Lee, M.; Lee, M.-H.; Rhee, S. B. *Synth. Met.* **1995**, *69*, 101.
(22) Kim, E.; Lee, K.; Rhee, S. B. *J. Electrochem. Soc.* **1997**, *144* (1), 227.
(23) Huguenin, F.; Giz, M. J.; Ticianelli, E. A.; Torresi, R. M. *J. Power Sources* **2001**, *103*, 113. Huguenin, F.; Torresi, R. M.; Buttry, D. A.; Pereira da Silva, J. E.; Cordoba de Torresi, S. I. *Electrochimica Acta* **2001**, *46*, 3555.
(24) Leroux, F.; Goward, G.; Power, W. P.; Nazar, L. F. *J. Electrochem. Soc*. **1997**, *144*, 3886.
(25) Willems, J. *Bull. Soc. Chim. Belg.* **1955**, *64*, 747.

Table 1. Chemical Compositions of LDH Organic Derivatives

sample	formula
$Cu_2Cr(OH)_6/Cl$	$Cu_{0.68}Cr_{0.32}(OH)_2\ Cl_{0.33}\cdot 0.75\ H_2O$[a]
H(**I**)	$Cu_{0.67}Cr_{0.33}(OH)_2(C_6H_4NH_2SO_3)_{0.32}Cl_{0.003}\ 0.68\ H_2O$
H(**II**)	$Cu_{0.67}Cr_{0.33}(OH)_2(C_6H_4NH_2SO_3)_{0.32}Cl_{0.003}\ 0.71\ H_2O$
H(**III**)	$Cu_{0.67}Cr_{0.33}(OH)_2(C_6H_3NH_2OCH_3SO_3)_{0.32}Cl_{0.003}\ 0.52\ H_2O$
H(**IV**)	$Cu_{0.67}Cr_{0.33}(OH)_2(C_6H_5NH(CH_2)_3SO_3)_{0.32}Cl_{0.003}\ 0.63\ H_2O$
H(**V**)	$Cu_{0.67}Cr_{0.33}(OH)_2(C_6H_5NH(CH_2)_4SO_3)_{0.32}Cl_{0.003}\ 0.55\ H_2O$

[a] Associated with an anionic exchange capacity of 286 meq per 100 g.

was aged overnight, centrifuged, and then washed several times with decarbonated water, and finally dried at room temperature. LDH chlorine form was synthesized in a similar way but in absence of the organic.

For the thermal treatment, the hybrid phase was placed in an open alumina crucible at 473 K for 4 h under an air atmosphere.

Elemental analyses (Cu, Cr, C, S, N, and H) were performed at the Vernaison Analysis Center of CNRS using inductive conduction plasma coupled to atomic emission spectroscopy (ICP/AES).

In the following, the hybrid phases will be noted as H(**X**), where **X** represents the organic molecule as shown in Figure 1.

Instrumentation. Powder X-ray diffraction profiles (PXRD) were obtained with a Siemens D500 X-ray diffractometer with a diffracted beam monochromator Cu Kα source. Steps of 0.04° with a counting time of 4 s were used. An X'Pert Pro Philips equipped with a HTK16 Anton Paar chamber and a PSD-50m Braun detector was used to record XRD diagrams at various temperatures. The conditions were step width of 0.0387°, time per step of 60 s, and aperture on 2° (155 channels).

Electron Spin Resonance. ESR spectra were recorded using an X Band Bruker EMX spectrometer equipped with a standard variable temperature accessory and operating at 9.653 GHz at room temperature and at 9.411 GHz when the temperature accessory was set up. Diphenylpicrylhydrazyl (DPPH) was used to determine the resonance frequency ($g = 2.0036 \pm 0.0002$) and the spin density (number of spins per gram of material).

Electrochemistry. Electrochemical measurements were performed by a three-electrodes cell with acetonitrile (ACN) and $LiClO_4$ (0.5 M) as electrolytes. The counter electrode and reference were platinum. The experiments were carried out under a potentiostatic mode with steps of 50 mV/s, and measured with a Princeton EGG-273 apparatus. The composite working electrode deposited on Pt grid was based on 80, 10, and 10% in weight of active material, carbon black, and poly(vinylidene difluoride), respectively.

3. Results

3.1 Characterization of the Hybrid Materials. From elemental analyses, the chemical compositions are reported in Table 1. The molar ratios Cu/Cr and S (or N)/Cu (or Cr) are close to the expected values, indicating that the reaction was complete between the metallic salts and that the organic moiety is entrapped in a quantity corresponding to the anionic exchange capacity of the obtained materials (Table 1).

3.1.1 X-ray Diffraction. The powder X-ray diffraction pattern of $Cu_2Cr(OH)_6Cl\cdot 2.25\ H_2O$ ($= Cu_{0.66}Cr_{0.33}(OH)_2Cl_{0.33}\cdot 0.75\ H_2O$) is characteristic of the layered double hydroxide structure (Figure 2). The pattern was refined using the $R\bar{3}m$ space group in rhombohedral symmetry. The cell parameters **a** and **c** (equal to three times the interlamellar distance) are equal to 0.311 and 2.315 nm, respectively.

The coprecipitation of the metallic salts in the presence of the organic molecules, (**I**)−(**V**), induces an increase in the basal spacing. There is no diffraction peak corresponding

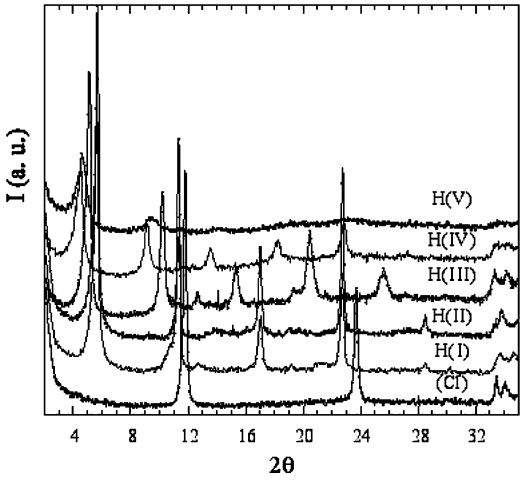

Figure 2. XRD patterns of $Cu_2Cr(OH)_6Cl$ LDH material and its organic derivatives.

to carbonate phase, suggesting that the incorporation of the guest molecule is completely achieved without such contamination. The coherence length along the stacking direction calculated from the Scherrer formula is $D_{hkl} = 0.9*\lambda/\beta_{1/2}\cos\theta$, in which λ is the X-ray wavelength, θ is the diffraction angle, and $\beta_{1/2}$ is the width at half-maximum intensity, which decreases as a function of the size of the organic molecule. A domain of ∼110 nm was found for the chlorine phase. It corresponds to ∼140 stacked layers, close to what is observed for other well-crystallized LDH materials.[26] This is slightly greater than that of the hybrid phase, 90 nm (corresponding to ∼60 stacked layers) for H(**I**), and much lower than that for H(**IV**) (50 nm). The width of diffraction lines for H(**V**) intercalated phase is out of validity for the Scherrer relation.

Concerning the local order, LDH host framework of cation composition Cu_2Cr presents a fairly high degree of local ordering.[27] In the case of the hybrid phases, the Fourier transform moduli at both Cu and Cr K-edge (not shown) exhibit features very similar to those of the chlorine LDH phase. The peaks of atomic correlations were refined at distances in agreement with a local order. Available on the short range only (sublattice diffraction peak is not observed), this structural local picture may be of interest to better understand the polymerization process in regard to the host (see discussion section).

In situ XRD patterns of the hybrid materials were recorded in air. The variation of the basal spacing is displayed in Figure 3. The corresponding thermal behavior is associated

(26) De Roy, A.; Forano, C.; El Malki, K.; Besse, J.-P. In *Synthesis of Microporous Materials* Occelli, L., Robson, H., Eds.; Van Nostrand Reinhold: New York, 1992; Vol. 2, p 108.
(27) Roussel, H.; Briois, V.; Elkaim, E.; de Roy, A.; Besse, J.-P. *J. Phys. Chem. B* **2000**, *104*, 5915.

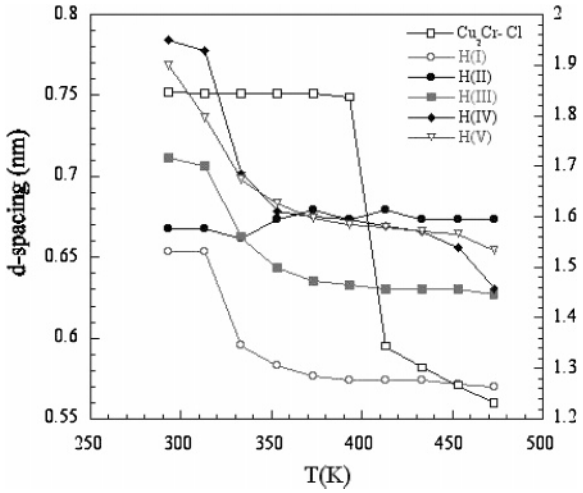

Figure 3. Variation of the basal spacing as a function of the temperature for $Cu_2Cr(OH)_6$ Cl LDH material and its organic derivatives.

with the dehydration and partial dehydroxylation of the hybrid materials. The basal spacing indicative of the confinement of the interlayered molecules decreases progressively until 350 K, and is constant above this temperature. This may be explained by a reorientation of the organic monomer and/or by an in situ polymerization. Few examples are found in the literature where the lamellar contraction is associated with the polymerization of the interleaved monomer such as for ϵ-aminocaproic acid to nylon into α-ZrP,[28] and acrylate,[29] α,β aspartate[17a] or styrene sulfonate[30] into hydrotalcite type compounds. ESR study will shed some light on the nature of the chemical process (see below).

At 450 K, the phase Cu_2Cr/Cl is partially degraded, and the compound Cu_2OCl_2 starts to form,[13c] whereas for the organic-intercalated phases, there is no byproduct until complete breakdown of the structure, which occurs at much higher temperature. This shows the benefit of the inorganic−organic assemblies in terms of structural stability in temperature, as previously underlined in other relative assemblies.[31]

3.1.2 ESR Experiments. In situ ESR measurements of the different hybrid materials were performed (Table 2). The corresponding spectra are displayed in Figure 4. At room temperature, all the ESR spectra of the hybrid materials exhibit a single Gaussian line with a peak-to-peak line width, noted as ΔH_{pp}, close to 1100 G ± 20 G and a Lande (g) factor of 2.0621 ± 0.0005. As underlined in a previous paper,[13c] the line shape is attributed to the combination of paramagnetic ions $Cu^{2+}(3d^9)$ and $Cr^{3+}(3d^3)$ in the material. The characteristics of ESR spectra are modified with the increase of the temperature, and become different from each other. Additional narrow signals are observed in some cases, which may be classified according to the Lande factor. For the hybrid phases H(**I**, **IV**, and **V**), the g value of the narrow signal ($g = 2.0034 \pm 0.0004$) is typical of organic radicals and/or conduction electrons. Since it is absent from the room-temperature spectrum, it has been attributed to the spin carriers localized along the organic structure. More detailed observations indicate that the narrow signal for H(**IV**) and H(**V**) was already present, but to a lesser extent, at room temperature; this suggests the presence of such a structure as soon as the hybrid materials are formed.

Table 2. Characteristics of ESR signals at 473 K

sample	ΔH_{pp} (G)[a]	g value (±0.0005)
$Cu_2Cr(OH)_6/Cl$	1100 ± 20	2.0621
(**I**), (**II**), (**III**), (**IV**) and (**V**)	no detectable	
H(**I**)	1100 ± 20	2.0621
	30 ± 2	2.0034
H(**II**)	1100 ± 20	2.0621
	15.4 ± 0.5	2.0048
	110 ± 5 (Cu^{2+})	2.0627
H(**III**)	1100 ± 20	2.0621
	15.2 ± 0.5	2.0046
	110 ± 5 (Cu^{2+})	2.0627
H(**IV**)	1100 ± 20	2.0621
	10.2 ± 0.5	2.0033
H(**V**)	1100 ± 20	2.0621
	15.6 ± 0.5	2.0034

[a] Peak to peak line width.

For the hybrid materials H(**II**), a signal resembles that of H(**I**) but it is much less pronounced. In contrast, there is no significant contribution for H(**III**). The temperature at which the narrow signal appears or increases is different among the hybrid materials. Qualitatively, the narrow signal is clearly observed at a temperature of 393 K for H(**I**) and H(**II**), and slightly higher (433 K) for H(**IV**) and H(**V**). To know if the formation of the organic structure is kinetically limited as observed for H(**I**), ex situ ESR measurements were performed after thermal treatment at 473 K for a longer time (not shown). After a period of time of 4 h, there is no significant variation of amplitude for the narrow signal. However, additional contributions are observed for H(**II**) and H(**III**). Their positions, $g \approx 2.06$ for the more intense line band, have to be interpreted by the presence of spin carriers localized onto the inorganic structure. To have more clues about their nature, the spectra were recorded at low temperature.

A broad asymmetrical line exhibiting a partially resolved hyperfine structure (hfs) is then observed (Figure 5a); it is assigned to isolated Cu^{2+} ions in an axially distorted octahedral environnement ($g_{\|} \approx 2.34$ and $g_{\perp} \approx 2.06$). Hfs is due to the interaction of the unpaired electron with the nuclear spin $I = {}^3/_2$ of the Cu^{2+} ion, even in a small amount.[32] These authors have observed that an increase in the cluster size of Cu^{2+} within glasses gives rise to linebands getting more and more symmetrical. In our case, this suggests that the domains of Cu^{2+} are rather small; their origin has to be understood by the partial degradation of the LDH matrix, thus forming CuO type phase at a nanometric scale. Such a presence is barely observed in the case of H(**I**), H(**IV**), and H(**V**). At this point, we conclude that the presence of an organic structure impedes the formation of CuO-type cluster

(28) Ding, Y.; Jones, D. J.; Maireless-Torres, P.; Rozière, J. *Chem. Mater.* **1995**, *7*, 562.
(29) Tanaka, M.; Park, I. Y.; Kuroda, K.; Kato, C. *Bull. Chem. Soc. Jpn.* **1989**, *62*, 3442. Rey, S.; Mérida-Robles, J.; Han, K.-S.; Guerlou-Demourgues, L.; Delmas, C.; Duguet, E. *Polym. Int.* **1999**, *48*, 277.
(30) Moujahid, El M.; Besse, J.-P.; Leroux, F. *J. Mater. Chem.* **2002**, *12*, 3324.
(31) Messersmith, P. B.; Stupp, S. *Chem. Mater.* **1995**, *7*, 454.
(32) Ardelean, I.; Peteanu, M.; Burzo, E.; Ciorcas, F. *Solid State Commun.* **1996**, *98*, 351. Ardelean, I.; Cozar, O.; Filip, S.; Pop, V.; Cenan, I. *Solid State Commun.* **1996**, *100*, 609.

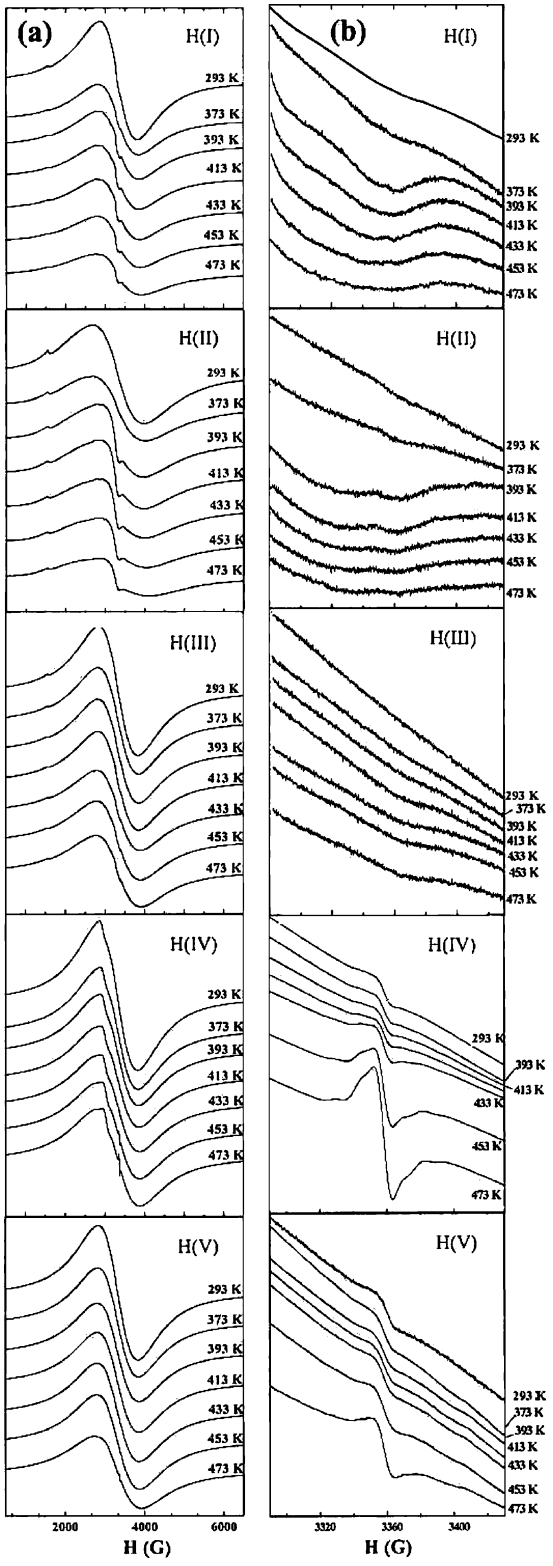

Figure 4. In situ ESR spectra of the hybrid materials in the temperature range 293−473 K recorded with a sweep width of (a) 6500 *G* and (b) 150 *G*.

in this temperature range. As clearly identified for other relative frameworks, it confirms here the stabilizing role of the organics for the lamellar structure when connected to each other.

Contrary to the narrow signal of H(**I**), which exhibits a single Lorentzian profile, the feature observed for H(**IV**) and H(**V**) is more intricate (Figure 5b); it is composed of the splitting into five lines indicating a superhyperfine structure (line denoted A in Figure 6). This phenomenon is due to the hyperfine interaction between localized spin and two neighboring nitrogen nuclei (nuclear spin $I = 1$) yielding to 5 lines ($2nI + 1$). The simulation of the signal leads to the hyperfine parameter $A = 12 \pm 1$ G, associated with a line width ΔHpp $= 12.0$ G $\pm$ 0.5 G and a g factor of 2.0033 $\pm$ 0.001. The line B results from the nonresolved hyperfine structure of the unpaired electrons interacting with the neighboring nitrogen and/or from another type of spin carrier with different localization within the organic structure.

The presence of such a hyperfine interaction implies that part of the unpaired electrons in the organic species are trapped in an environment composed of two nitrogen nuclei without delocalization. Observed in the case of H(**V**), the phenomenon is less evident than in the case of H(**IV**) (Figure 5b).

For the hybrids H(**IV**) and H(**V**), the spin carriers behave as isolated spin; this is evidenced by the evolution of the ESR parameters with temperature, and more precisely by the line width (ΔHpp) of the line B and its relative intensity (Figure 7a and b). Namely, the evolution of ΔHpp is independent of the temperature, and the intensity of the signal increases when decreasing temperature. This behavior is characteritic of Curie-type magnetism. The small curvature of the evolution noted on the curve intensity vs $1/T$ and observed in the higher temperature domain may be due to a component independent of the temperature. In contrast and as underlined previously, the positive temperature dependence of the ESR line width for H(**I**) is typical of conduction electrons as observed in conductive polymers.[33] Moreover, the corresponding intensity of the signal is then independent of the temperature, and has to be here interpreted by a Pauli-type mechanism.

3.1.3 Electrochemical Measurements. Previous works have shown that the inorganic framework may affect the electrochemical response of interleaved conductive polymer.[34] Since a large number of protons is necessary for the polymerization of aniline-based monomer, sulfuric acid is generally used for this process; unfortunately such a condition cannot be applied for LDH material. As reported by other authors, the polymerization of amino ring-substituted monomer may, however, be achieved in hydrophobic solvent.[35] Recently, it was also successfully demonstrated in hybrid LDH phases.[36]

(33) (a) Houzé, E.; Nechtschein, M.; Travers, J. P. *Phys. Rev. B* **1996**, *53*, 14309. (b) Kispert, L. D.; Joseph, J.; Miller, G. G.; Baughman, R. H. *J. Chem. Phys.* **1984**, *81*, 4. (c) Zhuang, L.; Zhou, Q.; Lu, J. *J. Electranal. Chem*. **2000**, *493*, 135. (d) Dubois, M.; Merlin, A.; Billaud, D. *Solid State Commun*. **1999**, *11*, 571. (e) Billaud, D.; Ghanbaja, J.; Marêché, J. F.; McRae, E.; Goulon, C. *Synth. Met*. **1989**, *28*, 147. (f) Rachdi, F.; Bernier, P. *Phys. Rev. B* **1986**, *33*, 11. (g) Mizoguchi, K.; Honda Kachi, N.; Shimizu, F.; Sakamoto, H.; Kume, K. *Solid State Commun*. **1995**, *96*, 333. (h) Feher, G.; Kip, A. F. *Phys. Rev. B* **1955**, *98*, 337.

(34) Widera, J.; Cox, J. A. *Electrochem. Commu.* **2002**, *4*, 118. Widera, J.; Grochala, W.; Jackowska, K.; Bukowska, J. *Synth. Met.* **1997**, *89*, 29. Ramachadran, M.; Lerner, M. M. *J. Electrochem. Soc*. **1997**, *144*, 3739. Phani, K. L. N.; Pitchumani, S.; Ravichandran, S. *Langmuir* **1993**, *9*, 2455.

(35) Yamada, K.; Teshima, K.; Kobayashi, N.; Hirohashi, R. *J. Electroanal. Chem.* **1995**, *394*, 71. Miras, M. C.; Barbero, C.; Haas, O. *Synth. Met.* **1991**, *43* (1−2), 3081.

(36) Moujahid, El M.; Dubois, M.; Besse, J.-P.; Leroux, F. *C. R. Chimie* **2003**, *6*, 2003.

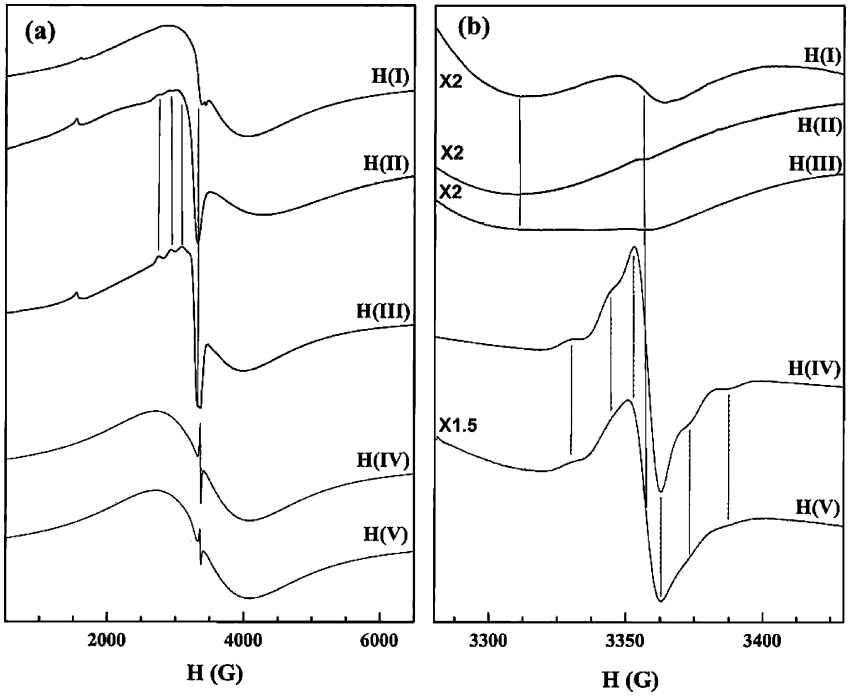

Figure 5. ESR spectra of the hybrid materials after treatment at 473 K for 4 h recorded at 105 K with a sweep width of (a) 6500 G (b) and 150 G.

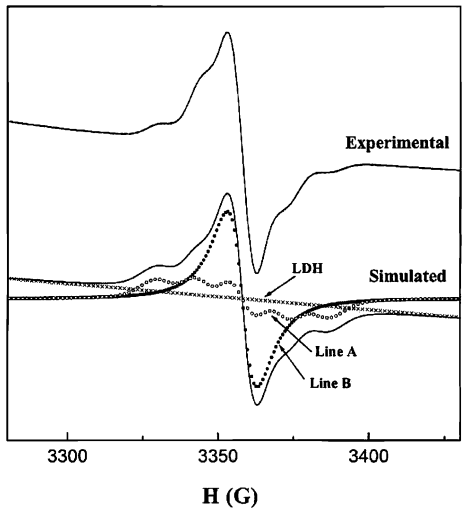

Figure 6. Simulation of the ESR spectrum recorded at 105 K of the phase H(**IV**) after a treatment at 473 K. The assignment of the lines is reported in the text.

The inorganic framework $Cu_2Cr-(Cl)$ LDH material exhibits a featureless capacitive response,[36] whereas redox peaks are observed in the case of the hybrid phase. The electrochemical behavior of (**I**) once incorporated into Cu_2-Cr is presented in Figure 8 a. After a few cycles, an anodic peak centered at −280 mV appears, it is associated with a peak at −550 mV during the cathodic sweep. Upon cycling, the intensity of these peaks increases, and the hysteresis decreases slightly between the 3rd and 10th cycles. The nature of these peaks is attributed to the formation of dimers, *p*-aminodiphenylamine. When further cycled, the sample presents an additionnal anodic peak located at −750 mV, characteristic of the response of oligomers of larger size and/or polymer (Figure 8 b).[37] Indeed, it is attributed to the quasi-reversible oxidation of leucoemeraldine to emeraldine.

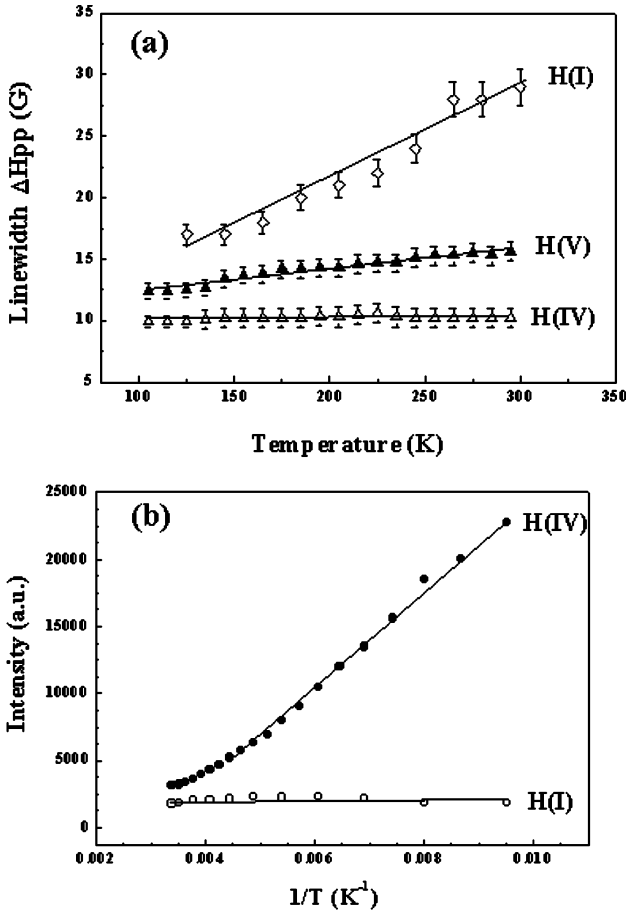

Figure 7. Variation of (a) the peak-to-peak ESR line width ΔH_{pp} vs T for H(**I**), H(**IV**), and H(**V**); and (b) ESR signal intensity vs $1/T$ for H(**I**) and H(**IV**).

After a thermal treatment at 200 °C for 2 h, there are significant differences in the electrochemical behavior, the

(37) Huang, W.-S.; Humphrey, B. D.; MacDiarmid, A. G. *J. Chem. Soc., Faraday Trans.* **1998**, *82*, 2385.

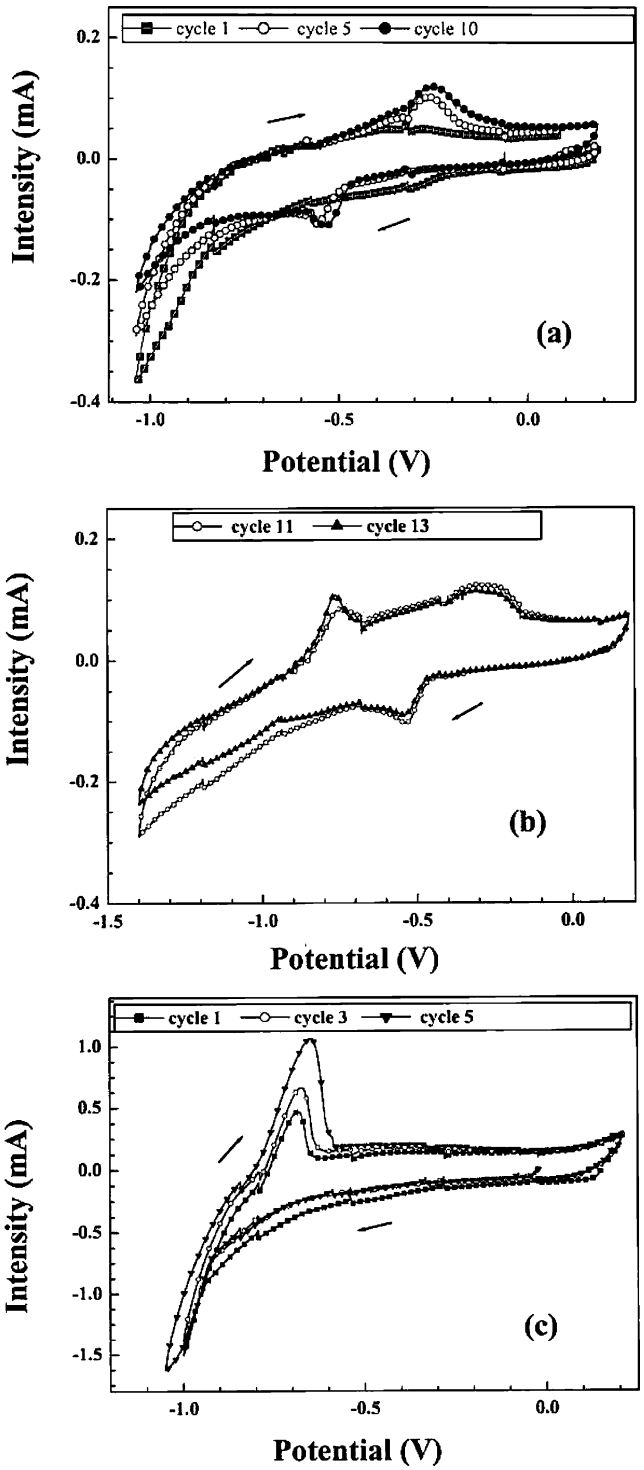

Figure 8. Cyclic voltammograms of H(**I**) (a) before treatment after 1st, 3rd, and 10th cycle, (b) 11th and 13th cycles, and (c) after thermal treatment at 473 K.

response of the dimers is not observed, and a well-defined anodic peak appears clearly on the voltammogram (Figure 8c). As previously observed in cycling for the same material without thermal treatment, its position at −700 mV (which is slightly shifted up to −650 mV after a few cycles) suggests the presence of polymer. Moreover, the absence of the electrochemical response of the dimers confirms the efficiency of the thermal treatment for the polymerization process. Correlatively, a larger spin density value is found for the cycled hybrid materials before thermal treatment

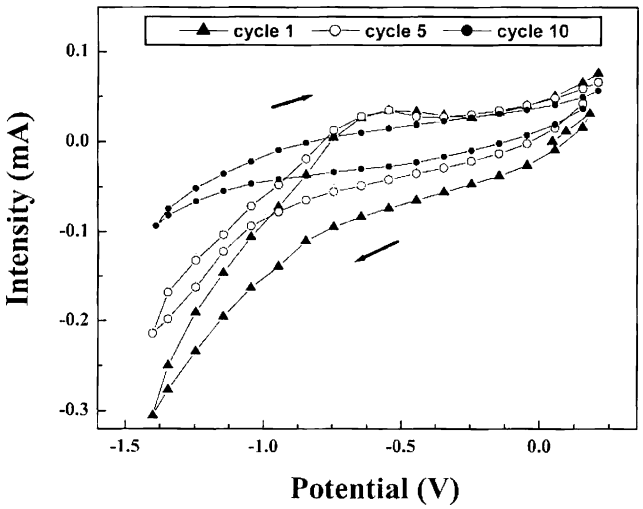

Figure 9. Cyclic voltammograms of H(**II**).

($2 \times 10^{18} \rightarrow 8 \times 10^{16}$ spin/g at the end of a few cycles in reduction process for the hybrid material before and after thermal treatment, respectively). The difference in the spin density is explained by the fact that spin carriers are localized on dimers rather than on larger polymer chains. In the same idea, a conductive polyaniline/clay hybrid system composed of montmorillonite as clay mineral showed *g* values higher than that of pure PANI, implying that the electrons are less free.[38]

Concerning H(**II**), there is no reversible redox process either before or after thermal treatment (Figure 9). This is in agreement with ESR study which has evidenced a very weak response of spin carriers probably present on the surface rather than located in LDH matrix.

For H(**III**) (Figure 10), the electrochemical curves features before and after thermal treatment are superimposed. A single peak is observed at −600 mV in oxidation, and a large cathodic hump is observed during the cathodic wave suggesting the presence of intricate electrochemical mechanisms. The apparent discrepancy with the ESR experiments, which indicate the absence of organic radicals, has to be understood by the difference of treatment. We surmise that the methoxy groups hinder the contraction of the lamellar structure in temperature and therefore the connectivity between monomer molecules as well, whereas the electrochemical treatment may change the initial state of the monomer, improving the affinity of the monomers to connect with each other. The response in the first cycles may be attributed to dimers, as the position of the peak is shifted toward lower potentials and its relative intensity decreases upon cycling.

The electrochemical curve features concerning the two hybrid materials H(**IV**) and H(**V**) are composed of single anodic peaks located at −200 and 0 mV, respectively. In both cases these redox peaks are shifted to higher potential upon cycling, and the cathodic peak is not well-defined, as exemplified by the electrochemical response of H(**IV**) before and after termal treatment (Figure 11). Since there is no other response upon cycling, we may attribute the anodic peak to the electrochemical response of the dimers observed by ESR

(38) Frisch, H. L.; Xi, B.; Rafailovich, M.; Yang, N.-L.; Yan, X. *High Perform. Polym.* **2000**, *12*, 543.

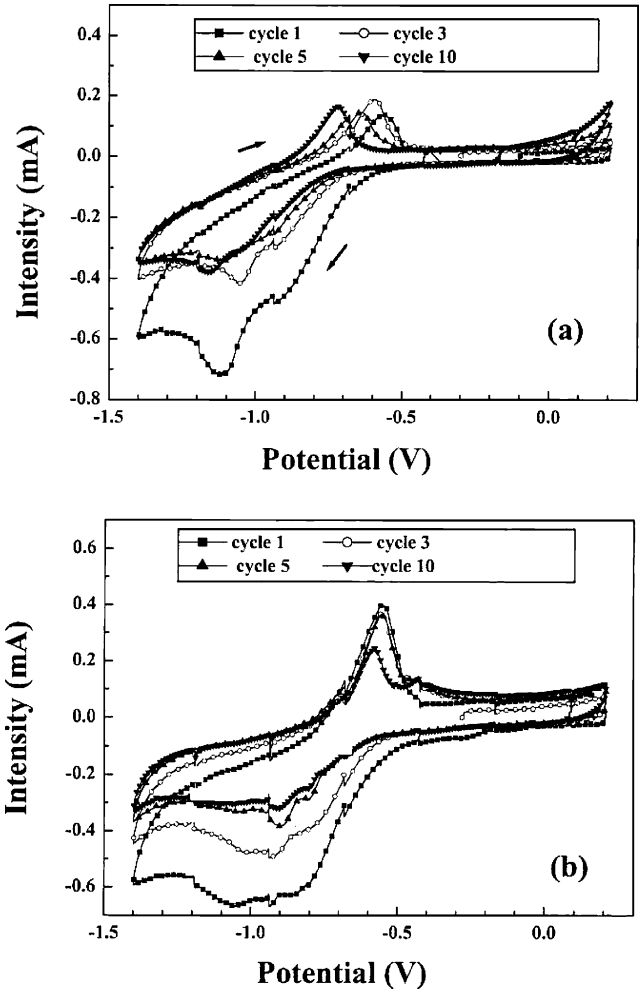

Figure 10. Cyclic voltammograms of H(**III**) (a) before and (b) after thermal treatment.

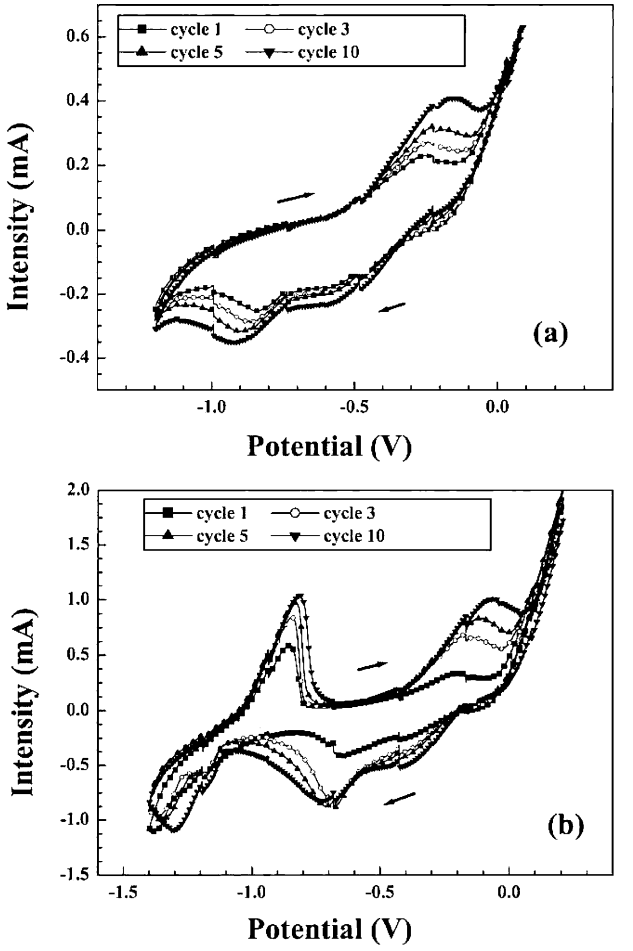

Figure 11. Cyclic voltammograms of H(**IV**) (a) before and (b) after thermal treatment.

experiments. The electrochemical response of the calcined hybrids is different (Figure 11b), and an additional well-pronounced signal is then observed. An anodic peak is located at −900 mV and at −1.3 V for its associated peak during the subsequent sweep, and the intensity of both peaks increases upon cycling. In comparison to the nonheat-treated sample, the signal may be associated to the spin carriers visualized by the line B in the refined ESR spectrum (Figure 6).

However, due to the lack of information in the literature concerning the electrochemical behavior of these relative organics, it is difficult to further ascertain the nature of the redox processes.

4. Discussion

In the following, the arrangement of the interleaved molecules and their subsequent dimerization and/or polymerization are discussed in term of the gap size and distances between localized charges.

Considering a local ordered structure and hydroxyl groups ideally packed, the charge are localized between each other at $\boldsymbol{a}\sqrt{3}$ and $3\boldsymbol{a}$ along different crystallographic directions, corresponding to distances of 0.54 and 0.91 nm, respectively.

However, the basal spacings for the organic incorporated phases range from 1.52 to 1.96 nm. Considering the dimension of the organic molecules estimated from electronic semiempirical Hartree−Fock calculations (Spartam program) and the dimension of the corrugated Cu_2Cr LDH, the experimental interlayer distances observed for the hybrid phases at room temperature are consistent for the presence of a bilayer of monomers in the interlamellar space, although, in highly constrained situation for some of them. It is accepted that the interlayer separation is not sufficient to unambiguously determine the arrangement of the guest molecule. It may be explained either by the double layer slightly tilted from an ideal perpendicular orientation in respect to the inorganic sheets or by molecules strongly interdigitated.

However, after thermal treatment, the lamellar structure is largely contracted, except for the material H(**II**) (Figure 3). The polymerization between monomer may proceed iso- or syndiotactically. In Figure 12, the expected basal spacings in the case of H(**I**) are reported. Considering the experimental data, it is obvious that the in situ polymerization evidenced by ESR and electrochemical characterizations proceed syndiotactically; the presence of a bilayer of polymer should induce a basal spacing ranging in 2.2 to 2.5 nm, much larger that the observed value (1.3 nm), whereas it is close to the case (b). Moreover, if we accept that the sulfonate groups are located according to the cation charge, the distance between monomers ranging from 0.59 to 0.64 nm is much larger than the distance $\boldsymbol{a}\sqrt{3}$ present in the layers. The

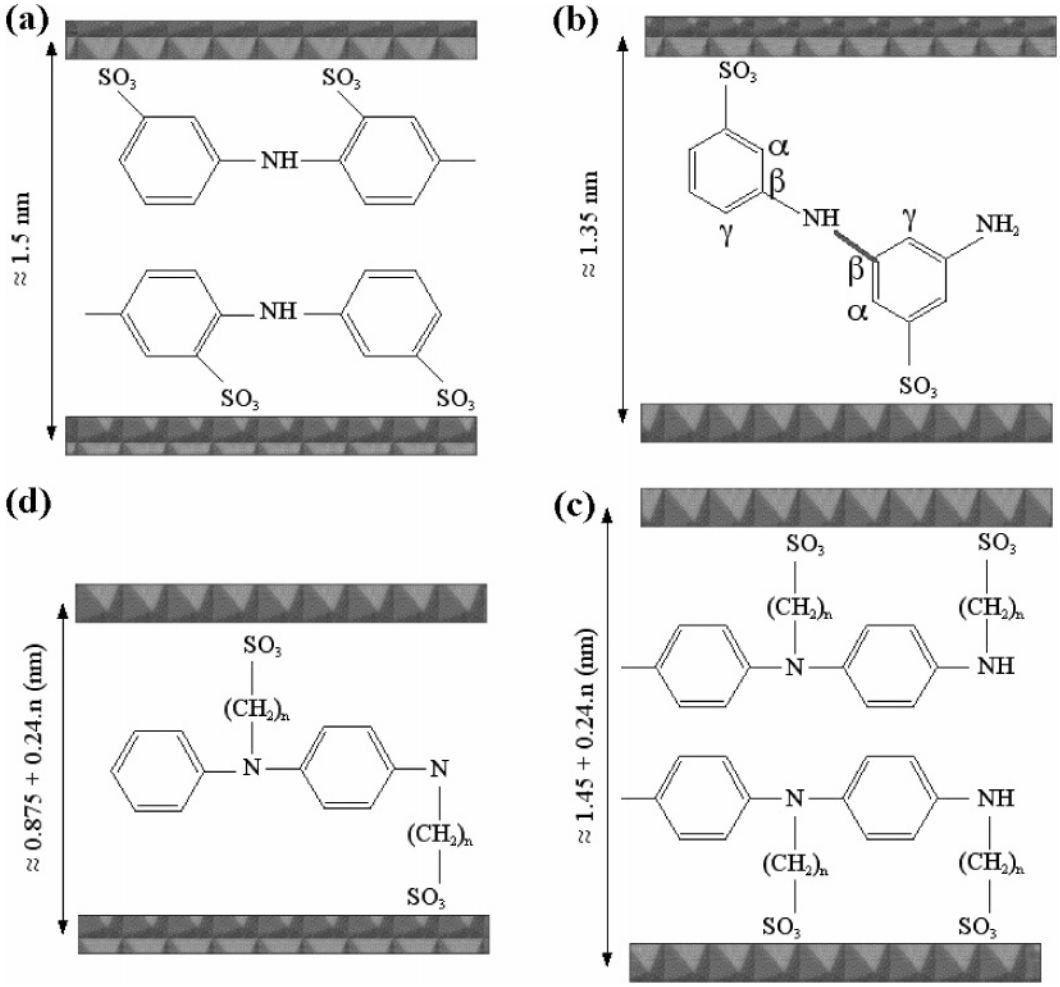

Figure 12. Schematic arrangement of the monomers connected either isotactically (a) and (c), or syndiotactically (b) and (d), using the hybrid materials H(**I**) and H(**IV**) as examples.

connection between monomer is likely to occur by a linkage (β, β) (Figure 12b). The propagation is not reachable either by a connection (β, γ) or (β, α), the latter should give rise to quasi-monolayer arrangement, not consistent with the experimental basal spacing.

Seemingly, the polymerization of (**II**) may proceed syndio or iso-tactically. The basal spacings expected in that case for the hybrid phase are 1.35 and 2.55 nm for a polymer disposed in monolayer and bilayer, respectively, whereas it is of 1.62 nm experimentally. Since the basal spacing is constant up to a temperature of 480 K, this suggests that no polymerization is occurring. We conclude that the polymerization is not favorable when the amino group is located in *o*-position from the sulfonate. This is in agreement with the ESR and the electrochemical studies.

For H(**III**), the presence of the methoxy group in *p*-position from the sulfonate hinders the polymerization process occurring in the case of H(**I**). Small amounts of dimers cannot be dismissed as depicted by ESR technique, since the interlayer distance is close to a favorable case for syndiotactic polymer (Figure 12 b) but not for a bilayer disposal.

For the phases H(**IV**) and H(**V**), the two calculated basal spacings reported in Figure 12c and d could explain a polymerization occurring in a syndiotactic way, and the observed contraction could be consistent with a highly interdigitated situation which should permit the polymer chain to propagate. Therefore we do not fully understand why such a process is limited as observed by the presence of the weak contribution (line B).

Nevertheless, a spontaneous dimerization is occurring for these hybrid phases. Similarly, a recent work reported the spontaneous polymerization of interleaved acrylate molecules into LDH deriving from $Ni(OH)_2$.[39] In our case, the lack of extended polymerization may be explained by the presence of dimers instantaneously formed. This tentative explanation suggests that the two monomers forming a dimer are located on a same inner side of the gap as no contraction of the basal spacing is observed at room temperature. Even present in a small amount, the dimers may hinder any further syndiotactic linkage between monomers of opposite inner side. Another explanation may be related to the electronic state of the interleaved molecules. Indeed, the polymerization takes place when the hybrid phase is electrochemically cycled. It shows that for a limiting factor for such a process to occur in a large extent may be electronic.

Finally, it is important to note when no polymerization happens, as for H(**II**), or when few dimers are sporadically

(39) Vaysse, C.; Guerlou-Demourgues, L.; Duguet, E.; Delmas, C. *Inorg. Chem.* **2003**, *42*, 4559. Vaysse, C.; Guerlou-Demourgues, L.; Duguet, E.; Delmas, C. *Macromolecules* **2004**, *37*, 45.

formed, as for H(**III**), the layer structure is then not stabilized and response of free cations Cu^{2+} is observed. Conversely, it underlines for the other three studied molecules the stabilizing effect not only at a long range order but also at the atomic scale since hfs of free cations Cu^{2+} is absent.

5. Conclusion

In light of the ESR and electrochemical measurements, the in situ polymerization of aniline-based monomer into a LDH structure, first evidenced on metanilic acid (**I**), is difficult to extend to other relative derivatives.

By means of ESR spectroscopy and also by indirect proof provided by electrochemical measurements, it was shown that the position of the amino (*ortho*) and presence of a methoxy group on the benzene ring inhibit the polymerization and that an alkyl chain spacer does not promote the degree of polymerization, as initially thought, but rather the dimerization.

In our early works, we surmised that the layer charge density was of great importance for such a process to occur. In view of these new results, the mechanism is more intricate and suggests that additional parameters need to be considered, such as the design of the guest molecule (its geometry and electronic configuration) associated with the ability of the lamellar structure to constrain or contract.

CM0401701